Article

Sulfonated Microporous Organic–Inorganic Hybrids as Strong Bronsted Acids

Zhike Wang, Joy M. Heising, and Abraham Clearfield

J. Am. Chem. Soc., **2003**, 125 (34), 10375-10383• DOI: 10.1021/ja030226c • Publication Date (Web): 31 July 2003

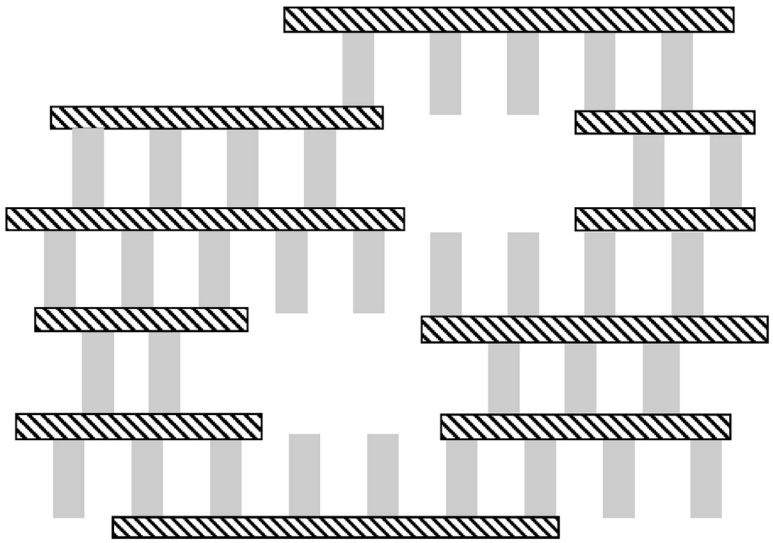

J|A|C|S
ARTICLES
Published on Web 07/31/2003

Sulfonated Microporous Organic−Inorganic Hybrids as Strong Bronsted Acids[1]

Zhike Wang, Joy M. Heising, and Abraham Clearfield*
Contribution from the Department of Chemistry, Texas A&M University, College Station, Texas 77842-3012

Received April 11, 2003; E-mail: Clearfield@mail.chem.tamu.edu

Abstract: It has been discovered that the use of excess zirconium in reactions with 4,4′-biphenyl and 4,4′-terphenylbis(phosphonic acid) in DMSO or DMSO−ethanol mixtures produces microporous inorganic−organic hybrids. Surface areas of 400 m^2/g and pore sizes in the range of 10−20 Å in diameter are routinely obtained. These materials are readily sulfonated with SO_3 under pressure to yield strong Bronsted acids. The acid strength, measured by ^{13}C NMR shifts of acetone and cyclopentanone in contact with the sulfonates, indicates an acidity close to that of 100% H_2SO_4. Condensation and cracking reactions were obtained for both ketones under mild conditions. A working hypothesis is presented to account for the high surface area and microporosity. The combination of high surface areas and pore dimensions that are between those of zeolites and mesoporous silicas commends these materials for applications in separations, ion exchange, and catalysis.

Introduction

Organic−inorganic hybrids constitute an important class of compounds in the exploratory research area of advanced materials design. In this connection, metal phosphonates represent a particularly versatile field for investigation because of the great latitude open to the investigator. A variety of di-, tri-, tetra-, penta-, and hexavalent metals readily combine with phosphonic acids. Furthermore, almost any desired organic compound may be converted into a phosphonic acid by known reactions. It is thus possible to introduce organics with different functional groups into the hybrid structure.[2]

Prior to the discovery of mesoporous silicas by Kresge et al.,[3] there was a concerted effort to prepare zeolites with larger pore openings so as to be able to effect catalytic reactions of large molecules within the pores or cavities. A detailed description of this effort is provided by Mark Davis.[4] Concurrent with this effort was the program to convert clay minerals, particularly smectites, into three-dimensional open porous materials by a process termed "pillaring". Briefly, the procedure consists of swelling the clay in water and then exchanging an inorganic polymer, such as the aluminum Keggin ion, $[Al_{13}O_4(OH)_{24}(H_2O)_{12}]^{7+}$, between the layers.[5,6] Upon heating above 500 °C, the pillars bond to the layers as permanent oxide pillars, producing a three-dimensional porous structure. An extensive literature on this subject exists of which the indicated references provide a good overview.[5−9] It was hoped that the pillaring procedure would produce uniform pores larger than 10 Å, but this has not been the case.

A detailed analysis[10] of a commercially prepared Al_{13} pillared montmorillonite (Laporte Absorbents) showed that about 50% of the pore volume was due to pores that are less than 10.9 Å in diameter, and the remainder of the pore volume resulted from pores with diameters of 10.9 to 20.8 Å. In contrast, an Al_{13} pillared sodium bentonite contained a small number of pores in the 7−11 Å range, the bulk in the 12−16 Å range, and mesopores arising from interparticle edge to face orientations.[11]

Alberti et al.[12] were the first to report the synthesis of zirconium phosphonates which included as one of the compounds layered zirconium phenylphosphonate, $Zr(O_3PC_6H_5)_2$. This compound was thought to have the same layer type as α-zirconium phosphate,[13,14] $Zr(O_3POH)_2 \cdot H_2O$, in which phenyl groups replaced the hydroxyl groups.[12] This supposition was shown to be correct when the crystal structure of the phenyl phosphate was solved using the powder X-ray data.[15] Dines et al.[16] conceived of the idea of producing porous materials by cross-linking the α-zirconium phosphate layers using diphos-

(1) Wang, Z. Ph.D. Dissertation, Texas A&M University, 2002.
(2) (a) Clearfield, A.; Wang, Z. *J. Chem. Soc., Dalton Trans.* **2002**, 2937. (b) Alberti, G. In *Solid State Supramolecular Chemistry and Layered Solids*; Alberti, G., Bein, T., Eds.; Pergamon Press: New York, 1996; Vol. 7, p 141. (c) Cao, G.; Hong, H.; Mallouk, T. E. *Acc. Chem. Res.* **1992**, *25*, 420. (d) Thompson, M. E. *Chem. Mater.* **1994**, *6*, 1168. (e) Clearfield, A. *Curr. Opin. Solid State Mat. Sci.* **1996**, *1*, 268. (f) Clearfield, A. In *Progress in Inorganic Chemistry*; Karlin, K. D., Ed.; John Wiley & Sons: New York, 1998; Vol. 47.
(3) Kresge, C. T.; Leonwicz, M. E.; Roth, W. J.; Vartuli, J. C.; Beck, J. S. *Nature* **1992**, *359*, 710,
(4) Davis, M. E. *Acc. Chem. Res.* **1993**, *26*, 111.
(5) *Catalysis Today*; Burch, R. Ed.; Special Issue on Pillared Clays; Elsevier Sci. Publ.: Amsterdam, 1990; Vol. 2.
(6) Clearfield, A. In *Advanced Catalysts and Nanostructure Materials*; Moser, W. R., Ed.: Academic Press: New York, 1996; pp 345−94.
(7) (a) Corma, A. *Chem. Rev.* **1997**, *97*, 2373. (b) Yang, R. I.; Cheng, L. S. In *Access in Nanoporous Materials*; Pinnavaia, T. J., Thorpe, M. F. Eds: Plenum: New York, 1995.
(8) Tomlinson, A. A. G. *J. Porous Mater.* **1998**, *5*, 259.
(9) Gil, A.; Gandia, L. M. *Catal. Rev.−Sci. Eng.* **2000**, *42*, 45.
(10) Molinard, A.; Clearfield, A.; Zhu, H. Y.; Vansant, E. F. *Microporous Mater.* **1994**, *3*, 109.
(11) Oliver, J. P.; Occelli, M. L. *J. Phys. Chem. B* **2001**, *105*, 623.
(12) Alberti, G.; Costantino, U.; Allulli, S.; Tomassini, N. *J. Inorg. Nucl. Chem.* **1978**, *40*, 113.
(13) Clearfield, A.; Smith, G. D. *Inorg. Chem.* **1969**, *8*, 431.
(14) Troup, J. M.; Clearfield, A. *Inorg. Chem.* **1977**, *16*, 3311.

10.1021/ja030226c CCC: $25.00

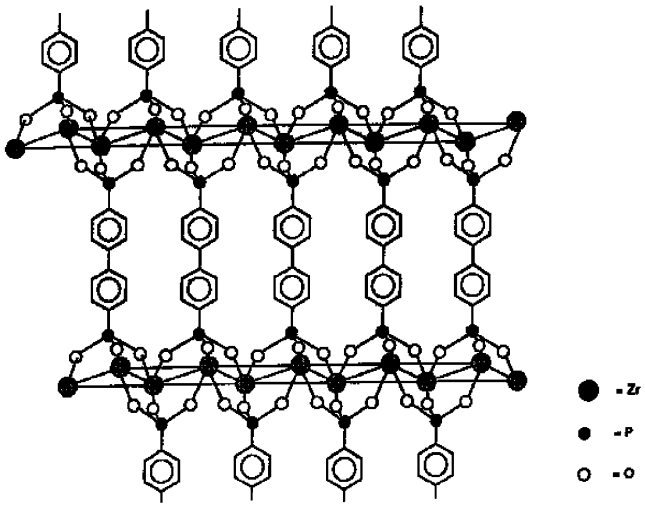

Figure 1. Schematic representation of idealized structure of zirconium biphenylenebis(phosphonate), $Zr(PO_3-Ph-Ph-PO_3)$.

phonic acids. The compound was depicted ideally as in Figure 1. Because the pillars would be only 5.3 Å apart, such materials should have no porosity. However, by introducing spacer molecules such as phosphorous acid, the Dines group[16] was able to obtain porous "house of cards" type products. Unfortunately, they did not measure the pore size distribution. Subsequent work has shown that if the reactions are carried out in aqueous media, the pore size distribution is very broad and mainly of the mesoporous type.[17,18]

One of the interesting results reported by Dines et al.[16] was the fact that even the fully pillared compound, in which no spacer group was added, exhibited a very high surface area. Alberti et al.[18,19] proposed that all the surface area was a result of edge to face stacking of very small particles to produce mesoporosity. However, subsequent work by us showed that considerable microporosity can develop in the particles prepared in DMSO and that the particles are too large to have such large surface areas formed totally from outer particle surfaces.[20,21] Our goal, however, was to obtain pores with diameters in the 10−20 Å range. This region is just the one where zeolites leave off and the mesoporous materials sorbents for separation procedures of intermediate begin. Not only would this development yield sorbents for separation procedures of intermediate sized molecules, but sulfonation of the phenyl rings should produce highly acid catalysts for effecting transformations of large molecules that enter the cavities. In this paper, we report that significant progress has been made toward that goal.

Experimental Section

Reagents. Zirconyl chloride octahydrate (98%), zirconium sulfate hydrate (99.99%), dimethyl sulfoxide (99.9%), fuming sulfuric acid (26.0−29.5% SO_3), and methyl-^{13}C alcohol (99%) were obtained from Aldrich. Hydrofluoric acid (48%) was purchased from Mallinckrodt. Acetone-2-^{13}C (99+%) and pyridine-^{15}N (99+%) were obtained from Isotec. Cyclopentanone-1-^{13}C (99.9%) was purchased from Cambridge Isotope Labs. All isotope-labeled reagents were purified via several freeze−pump−thaw cycles. Other reagents were used as purchased without further purification.

Preparation of 4,4′-Biphenylenebis(phosphonic acid), BPBPA. The diethyl ester of the desired acid was prepared by a slightly modified Arbusov reaction.[22] 4,4′-Dibromobiphenyl (6.27 g, 20 mmol) and 50 mL of 1,3-diisopropylbenzene were added to a 250-mL three-neck flask, fitted with a reflux condenser, N_2 inlet, and an addition funnel. The solution was heated to 185°C, and 0.50 g of $NiBr_2$ was added as a catalyst. The flask was purged with N_2, and 10 mL triethyl phosphite (Aldrich) was added over a 6-h period under a gentle stream of N_2. The mixture was refluxed for 24 h followed by the addition of 0.25 g of $NiBr_2$ and 5 mL of triethyl phosphite. The mixture was heated for another 24 h, and the cooled black solution was distilled under vacuum to remove the solvent and unreacted triethylphosphite. The solid was extracted with petroleum ether and then recrystallized from methylene dichloride and petroleum ether. This ester was converted to the corresponding diphosphonic acid by refluxing in HCl. Yield 5.04 g (80%). ^{31}P NMR spectra (H_3PO_4 as external standard) of a concentrated solution of the hydrolysate showed a single resonance at 14.8 ppm.

Preparation of Zirconium 4,4′-Biphenylenebis(phosphonate), ZrBPBP. The general procedure was to react $ZrOCl_2 \cdot 8H_2O$ complexed by HF with the diphosphonic acid at temperatures of 80 °C in a hydrothermal reaction vessel. The solvent was dimethyl sulfoxide, DMSO, or a mixture of DMSO and ethanol. In some preparations, H_3PO_4 was added as a spacer group. The phosphoric acid was always combined with the phosphonic acid before adding the zirconium solution. This was done to prevent premature formation of a zirconium phosphate phase.

Preparation in Mixed Ethanol−DMSO Solution (Sample II-9). 4,4′-Biphenylenebis(phosphonic acid) (1.03 g, 3.28 mmol) was dissolved in a mixture of 100 mL of ethanol (95%) and 25 mL of DMSO. A mixture of 2.172 g of $ZrOCl_2 \cdot 8H_2O$ (6.72 mmol) and 4.24 mL of 48% HF (121 mmol) in 100 mL of ethanol was slowly added to the phosphonic acid solution. This mixture was transferred to a Teflon-lined pressure vessel and kept at 80 °C for 3 days. The solid precipitate was then recovered by centrifugation, washed free of chloride and fluoride ions, and dried at 50 °C. Yield 0.993 (70%). Anal. Calcd for $Zr(O_3PC_{12}H_8PO_3)_{0.74}(H_2O_3PC_{12}H_8PO_3)_{0.275}F_{0.49} \cdot 0.88H_2O$: 21.28% Zr, 14.67% P, 34.12% C, 2.45% H, 2.17% F, 3.7% H_2O. Found: 21.12% Zr, 14.57% P, 33.85% C, 2.71% H, 2.17% F, 3.69% H_2O (TGA).

Synthesis of 4,4′-Dibromoterphenyl. The synthetic procedure used was a modification of one reported earlier.[23] Terphenyl (10 g, 43 mmol) was dissolved in 70 mL of bromobenzene with heating to 130 °C. A trace of I_2 was added as a catalyst, and then 4.7 mL of Br_2 (86 mmol) were added dropwise. When the color began to lighten, an additional trace of I_2 and 3 mL of Br_2 were added. Heating was continued for 2 more days, then the mixture was cooled, and the solid filtered and washed with a sodium thiosulfate solution. Yield 11.5 g (68.2%). The dried product contained 41% Br (41.2% calculated).

Synthesis of Zirconium 4,4"-Terphenylenebis(phosphonate), ZrTPBP. The dibromoterphenyl was converted to the corresponding phosphonic acid by the Arbusov reaction followed by the hydrolysis as described for the bipheylenedibromide. To a solution of 2 g of $ZrOCl_2 \cdot 8H_2O$ (6.6 mmol) in 120 mL of DMSO was added 4 mL of HF (124 mmol). A separate solution of 1.2 g (3.08 mmol) of 4,4"-terphenylenebis(phosphonic) acid in 60 mL of DMSO was prepared, and both solutions were transferred to a Teflon-lined pressure vessel and kept at 80 °C for 3 days. The solid was recovered by filtration, washed free of Cl^- with water, and dried overnight at 50 °C. Anal.

(15) Poojary, M. D.; Hu, H. L.; Campbell, F. L., III.; Clearfield, A. *Acta Crytsallogr.* **1993**, *B49*, 996.
(16) Dines, M. D.; Di Giacomo, P. M.; Callahan, K. P.; Griffith, P. C.; Lane, R. H.; Cooksey, R. E. In *Chemically Modified Surfaces in Catalysis and Electrochemistry*; Miller, J. S., Ed.; ACS Symposium Series 192; American Chemical Society: Washington, DC, 1982; Chapter 12.
(17) Clearfield, A. In *Design of New Materials*; Clearfield, A., Cocke, D. A., Eds.: Plenum Press: New York, 1986, pp 121−134.
(18) Alberti, G.; Costantino, U.; Vivani, R.; Zappelli, P. *Mater. Res. Soc. Symp. Proc.* **1991**, *233*, 101.
(19) Alberti, G.; Marmottini, F.; Vivani, R.; Zappelli, P. *J. Porous Mater.* **1998**, *5*, 221.
(20) Clearfield, A. *Chem. Mater.* **1998**, *10*, 2801.
(21) Clearfield, A.; Wang, Z.; Bellinghausen, P. *J. Solid State Chem.* **2002**, *167*, 376.
(22) Harvey, R. G.; Desombre, E. R. *Top. Phosphorus Chem.* **1964**, *1*, 57.
(23) Bellinghausen, P. M.S. Thesis, Texas A&M University, Dec. 1995.

Table 1. Experimental Conditions and Product Texture of Zirconium Biphenylenebis(phosphonates), $T = 80$ °C, 3 Days

sample no.	reactant ratios Zr:BPBPA[a]:H_3PO_4:HF	solvent	product ratios P:Zr:F	SA (m^2/g)	micro SA (m^2/g)	vol micropore cc/g	micropore diameter maxima (Å)
II-6b	2:1:6:120	DMSO	2.29:1:0.18	107	28	0.051	11
II-6a	2:1:10:130	DMSO	2.31:1:0.18	156	121	0.059	8
II-6e	2:1:20:120	DMSO	2.15:1:0.14	109	78	0.055	11,15
II-26c	2:1:6:40	DMSO	1.95:1:0.44	371	363	0.232	13
II-6 g	2:1:0:35	DMSO	2.09:1:0.37	406	381	0.199	17−19
II-6h	2:1:0:35	DMSO/EtOH 4:1	2.12:1:0.38	395	370	0.193	16−18
II-8b	2:1:0:40	DMSO/EtOH 1:4	2.01:1:0.47	410	396	0.279	14−16
II-9	2:1:0:40	DMSO/EtOH 1:8	2.03:1:0.49	416	401	0.268	13
28a[b]	2:1:0:12	DMSO	1.70:1:0.76	410	401	0.254	13

[a] 4,4′-Biphenylenebisphosphonic acid, $H_2O_3PC_6H_4C_6H_4PO_3H_2$. [b] Temperature was 120 °C.

Calcd for $Zr(O_3PC_{18}H_{12}PO_3)_{0.65}(H_2O_3PC_{18}H_{12}PO_3)_{0.29}F_{0.82}\cdot 0.65H_2O\cdot$ 0.38DMSO: 17.82% Zr, 11.38% P, 41.48% C, 3.04% H, 3.04% F. Found (Sample 24b): 17.78% Zr, 11.33% P, 41.63% C, 3.23% H, 3.05% F. The water and DMSO contents were obtained from the TGA which gave weight losses of 2.37% to 100 °C, 5.90% from 100 to 417 °C, and 40.64% from 417 to 720 °C.

Sulfonation of Zirconium Bi- and Terphenylenephosphonates. ZrBPBP (0.5 g) was placed into a 40-mL Teflon-lined pressure vessel along with 2 mL of fuming sulfuric acid (26.0−29.5% SO_3) contained in a glass tube. The sealed vessel was then kept at 150 °C for 6 days. The cooled vessel was opened in a plastic airbag purged with dry N_2, and the sulfonated solid was transferred to a dry vial, sealed with wax, and stored in a nitrogen-purged glovebox for later use. Two samples of II-9 were sulfonated. Sample 22 treated for 6 days contained 8.74% S or 0.714 SO_3H groups per ring and 22B treated for 3 days contained 3.86% S or 0.28 SO_3H per ring.

A terphenyl sample, II-24b, was treated for 6 days as indicated above for the biphenyl compounds resulting in incorporating 15.5% S which amounts to 4 mol of SO_3. This amount is equivalent to 1.32 SO_3H groups per phenyl ring. It is sample II-25.

Surface Area Measurements. Sorption−desorption isotherms were obtained with a Quantachrome Autosorb-6 automated N_2 gas adsorption unit. The samples (0.2−0.6 g) were preheated at a temperature of 200 °C under the vacuum on the Quantachrome degasser until a pressure of 2×10^{-3} Torr was achieved. The isotherms were obtained at 77 K and analyzed by the BET model. The micropore volume was determined by the DeBoer t-plot method, and the micropore distribution was calculated by the MP method.

Analytical and Instrumental. Zirconium and phosphorus analysis was carried out in-house with a Direct Current Plasma (DCP) spectrometer. A weighed portion of the sample was dissolved in 1 mL of 48% HF with heating and then diluted to 200 mL. Aliquots were then removed and diluted to a composition falling well within the standard curves for Zr and P, respectively. Samples that did not dissolve in HF were heated to 500°C in air for 10h to destroy the organic. The residue was then dissolved in HF and diluted as before. Alternatively, these elements and F were determined using a Cameca 5×50 electron microprobe at an accelerating voltage of 15 kV and operating with a beam current of 20 mA using a wavelength-dispersive spectrometer (WDS). C, H, S analyses were performed by Galbraith. Thermogravimetric analyses were conducted on a TA 950 unit at a heating rate of 3 to 10 °C/min under a flow of air. Solid state MAS NMR measurements were obtained on a modified Bruker MSL-300 MHz spectrometer operating at 121.5 MHz for ^{31}P, 75.4 MHz for ^{13}C, and 30.42 MHz for ^{15}N. 85% H_3PO_4, 0 ppm, adamantane, 38.3 ppm, and glycine, 36.5 ppm were used as external chemical shift standards for ^{31}P, ^{13}C and ^{15}N, respectively. All ^{13}C chemical shifts are reported relative to tetramethylsilane (TMS), whereas ^{15}N chemical shifts are relative to NH_3. X-ray powder patterns were obtained on a Seiferth−Scintag PAD-V unit with Cu Kα ($\lambda = 1.5418$ Å) at 40 kV and 30 mA. TEM micrographs were recorded using a JEOL 2010 operating at 200 kV. SEM images were acquired using an Electroscan ESEM E-3 at an accelerating voltage of 15 kV and a pressure of 5 Torr.

Catalyst Sample Preparation and MAS NMR. The following procedure was used for preparing samples with a probe molecule adsorbed on the catalyst surface. All preparations were conducted under inert atmosphere or vacuum conditions. Typically, ∼0.25 g of catalyst was loaded into a glass tube in a glovebox, sealed by stopcocks, and removed from the glovebox and connected to a vacuum line. The catalyst was kept under vacuum overnight, and usually the final pressure was less than 2×10^{-4} Torr. Adsorptions of organic molecules were primarily conducted at room temperature, after which each sample was transferred into an NMR rotor inside a nitrogen-purged glovebox. Typical ^{13}C experiments included the following: cross-polarization (CP, contact time = 1 ms, pulse delay = 1 s, 2000−16 000 transients); single pulse excitation with proton decoupling (Bloch decay, pulse delay = 20 s, 200−4000 transients). ^{15}N experiments included the following: cross-polarization (CP, contact time = 1 ms, pulse delay = 2 s, 4000 transients); single pulse excitation with proton decoupling (Bloch decay, pulse decay = 10 s, 4000 transients). All the spectra shown were obtained with Bloch decay experiments, except where otherwise stated. Zirconia rotors (7.5 mm) were spun at typically 2−5 kHz.

Table 1 summarizes the conditions of reactions and some results for a number of the preparations of the biphenyl derivatives. Three variables were explored, the ratio of HF to Zr, the addition or nonaddition of H_3PO_4 as a spacer group and the solvent composition. We had shown earlier that use of DMSO as solvent produced porous pillared materials with about 50% of the pores in the micropore region.[20] The difference in the present study is the fact that an excess of Zr relative to the diphosphonic acid was employed. The reason for this Zr excess will be presented later.

Results

Zirconium Biphenylphosphonates. All the samples for which the HF:Zr ratio was 20 or less had surface areas of the order of ∼400 m^2/g with more than 90% of the surface area accounted for as micropores. For those samples where the HF:Zr ratio was higher, the surface area was considerably lower. Furthermore, these samples contained a higher proportion of mesopores and they exhibited a greater range of pore sizes. In the case of samples 6a, b, and e, the diminished surface area and unfavorable pore size distribution might be attributed to the addition of phosphoric acid. However, the results with sample 26c, for which both high surface area and narrow pore size distribution were obtained, refute this possibility. Therefore, we attribute the differences in the results to the high level of HF in the low surface area samples. Increasing the ratio of ethanol to DMSO (samples 6h, 8b, 9h) did not greatly change the sample texture. All of these samples gave satisfactorily high surface areas and narrow pore size distributions. However, the use of alcohol prevented the formation of colloidal dispersions that are common when DMSO is the solvent. As a result, less troublesome recovery of the product was achieved.

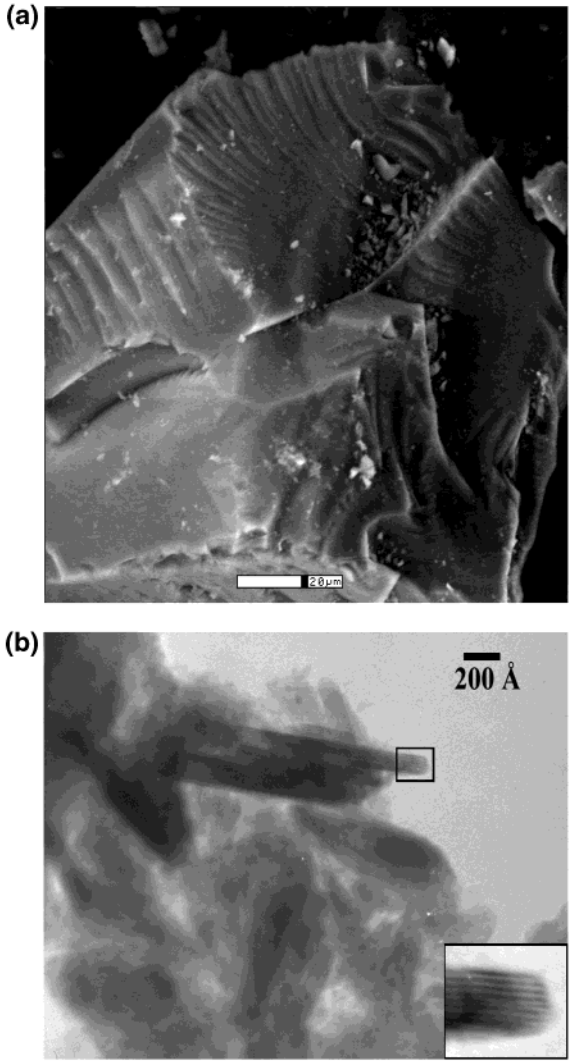

Figure 2. (a) Scanning electron micrograph (SEM) of the sample ZKW-II-9. (b) TEM of a ground sample of II-9. The inset shows a portion of an individual particle containing eight layers.

The X-ray powder diffraction patterns for sample II-9 show initial *d* spacings of 13.65 and 14.13 Å for the unsulfonated sample and sulfonated states. The interlayer spacing of 13.65 Å is expected from consideration of the layer thickness, 6.6 Å, and the length of the biphenyl pillar, ~7 Å. Upon sulfonation, a slight increase (~0.5 Å) in the interlayer was observed. This increase may well result from water intake into the cavities upon exposure to the atmosphere. Only two or three additional broadened reflections are observed at a higher angle, indicative of the semicrystalline nature of the products. The major reflections are of the (00*l*) type indicative of layered compounds in which the ZrO_6 layers are cross-linked by the biphenyl groups.

Scanning electron micrographs reveal particles in the 10−100 μm range and a host of fragments of submicron sizes. The particles exhibit no regular crystalline shape. However, as seen in Figure 2a, the large particles appear as though they are built up of a series of platelike particles that have bonded together. A transmission electron micrograph taken of a well-ground sample revealed the existence of groups of nanocrystals (Figure 2b). An enlargement of a portion of the sample (Figure 2b) reveals that some of the individual particles are about 8 layers thick (~100 Å). A group of three such particles appear to be stacked on top of each other to form a single particle that is about 30 nm thick and ~120 nm long. Thus, the large particles observed by SEM must arise from the bonding together of platelets along their flat surfaces.

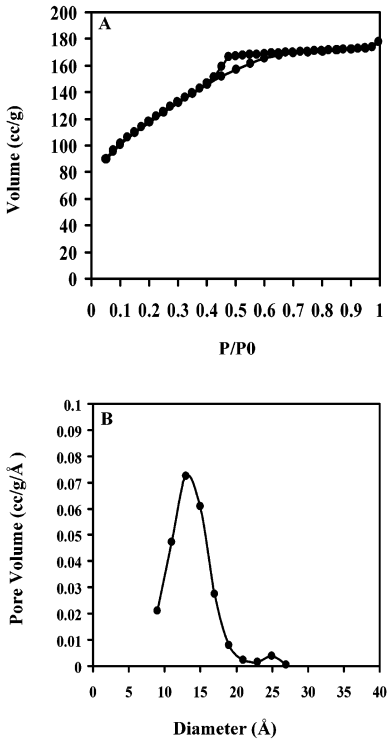

Figure 3. (A) N_2 adsorption−desorption isotherm and (B) pore distribution of the sample ZKW-II-9 prepared in DMSO and ethanol.

Figure 3 presents an N_2 sorption−desorption isotherm and the pore size distribution from analysis of the curves. It is seen that the micropores are wholly within the 10−20 Å range, and therefore, these materials fill the gap between zeolites whose useful channel sizes are 10 Å or below and the mesoporous materials, which cover the 20−100 Å range. The isotherms are of type IV in the BDDT classification[24] and exhibit a hysteresis indicative of slit-shaped pores.

Derivation of Formulas for the Porous Pillared Zirconium Phosphonates. Normally, the derivation of formulas for zirconium phosphonates is straightforward. However, certain complications arise in connection with the porous pillared materials. These complications result from the necessity to account for phosphorus−zirconium ratios of greater than two[25] and the presence of fluoride ion in the samples. A combination of elemental and thermogravimetric analyses was utilized, as detailed below for sample II-9, for all the samples.

The thermogravimetric weight loss curve for sample II-9 gave a total weight loss of 37.04%, and the end product was ZrP_2O_7, formula weight 265.2 g. Dividing this value by the fraction remaining at 1000 °C (0.6296) provides a provisional formula weight of the initial solid, 421.2 g. Because of the presence of 0.49 mol of F, which we assume is bonded to Zr, the ratio of phosphorus to Zr should be less than 2. It is, in fact, 2.03 (Table 1). The only way the ratio can achieve this value is for a fraction

(24) Gregg, S. J.; Sing, K. S. W. *Adsorption, Surface Area and Porosity*, 2nd ed.; Academic Press: New York, 1982; p 4.
(25) Alberti, G.; Costantino, U.; Vivani, R.; Zappelli, P. *Mater. Res. Soc. Symp. Proc.* **1991**, *233*, 101.

Table 2. Experimental Conditions and Product Texture of Terphenylenebisphosphonates (ZrTPBP), $T = 80°C$, 3 Days

sample no.	reactant ratios Zr:TPBPA:HF	solvent	product ratios P:Zr:F	SA (m^2/g)	pore structure: micro SA (m^2/g)	pore structure: vol micropore (cc/g)	pore structure: micropore diameter (Å)
23C	2:1:40	DMSO	2.12:1:0.45	407	395	0.294	12−17
23B	2:1:40	DMSO	1.96:1:0.63	357	345	0.229	11−16
24b	2:1:40	2EtOH/DMSO	1.88:1:0.82	273	269	0.150	11
29	2:1:80	DMSO	2.02:1:0.85	301	295	0.167	11−13

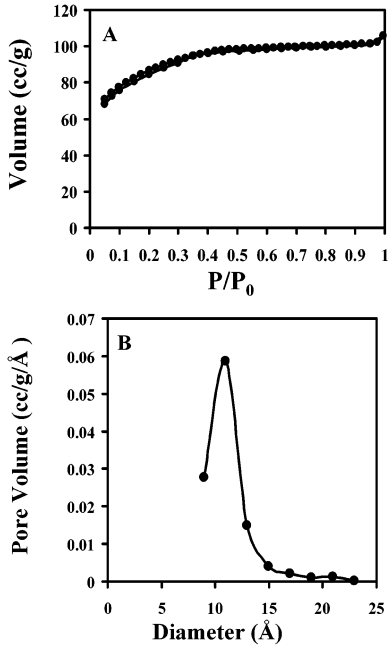

Figure 4. (A) the N_2 adsorption−desorption isotherm and (B) pore distribution of the **ZrTPBP** sample ZKW-II-24b.

of the biphosphonic acid to be bonded to the layers through only one phosphonic acid group. In fact, almost all the samples in Table 1 have P:Zr ratios higher than 2. The conditions to be fulfilled are the charge balance and P:Zr ratio, 2.03. Let x equal the doubly bound phosphonate groups and y the singly bound value. Charge balance requires $4x + 2y + 0.49 = 4$, and the ratio P/Zr is $2x + 2y = 2.03$. Solution of these equations leads to $x = 0.74$, $y = 0.275$, to give the proposed formula in the experimental for this sample. We note that although the P/Z is close to 2, 27% of the diphosphonic acid groups are bonded to the layers through only one acid group. This large number of singly bound groups is partly the result of sites on the layer occupied by fluoride ion, which prevent cross-linking by the diphosphonic acid. However, it is not the only reason as discussed later.

Zirconium Terphenyl Derivatives. Table 2 summarizes the synthesis conditions for the pillared terphenyl compounds. The results for these derivatives show comparably high surface areas with narrow pore size distributions in the 10−20 Å range. A typical isotherm and its micropore distribution are given in Figure 4. It should be noted that the isotherm features are more like that of a type I microporous compound except for a slight upturn very near a partial pressure of 1. There is also a significant decrease in surface area for samples II-24b and II-29. This decrease is attributed to the use of ethanol for the former sample and the presence of a higher amount of HF in the preparation of the latter sample. We have already seen in the case of the biphenyl derivatives that the use of high HF levels is not desirable. Why the use of alcohol in the solvent mix in this case reduces the surface area (SA) requires further study.

Sulfonation of the Zirconium Arylphosphonates. Immersion of the pillared porous materials in fuming sulfuric acid results in sulfonation of the phenyl rings.[26] However, recovery of the sulfonate involves partial neutralization of the acid, filtration, and extensive washing. It is then difficult to obtain totally anhydrous material without loss of some SO_3.

For our purposes, the measurement of the acid strength of the SO_3H groups, it was essential to obtain moisture-free samples. Therefore, we utilized a procedure to sulfonate the rings with gaseous SO_3 under pressure. The dry powder was then transferred to the reaction vessel in a drybox, and the nature of the acid sites and their acid strength was determined as detailed below. Three such samples were prepared. Two biphenylsulfonates containing respectively 3.86% and 8.74% S (0.27 and 0.714 SO_3) and one terphenyl derivative with 15.5% S or 1.32 SO_3 groups per ring.

Nature of Acid Sites. To determine the nature of the acid sites in S-ZrBPBP, pyridine-^{15}N was used as a probe molecule. The common procedure is to sorb the pyridine and then observe the IR bands at 1450 and 1540 cm^{-1} for the presence of Lewis and Bronsted acid sites, respectively. However, Maciel and Haw et al.[27,28] showed that the sorbed pyridine produces different ^{15}N chemical shifts for the two acid types. The pyridinium ion generated in the zeolite HZSM-5 has an isotropic chemical shift of 208 ppm, and the pyridine−Lewis acid complex on anhydrous $AlCl_3$ produced shifts of 226 and 235 ppm.[29] Aluminum chloride supported on silica is a very strong Bronsted acid and produces a chemical shift of 196 ppm in ^{15}N. The in situ NMR solid state MAS spectrum for ^{15}N-pyridine on the 8.74% S biphenyl derivative is shown in Figure 5. Both the cross-polarization and single pulse Bloch decay spectra show that all the pyridine exists as pyridinium ion on Bronsted acid sites with the shift being 203 ppm. This chemical shift remains constant on increasing the loading from 0.4 to 0.71 mmol/g. The fact that neither the chemical shift nor the line shape of the resonance changes on increased loading indicates that the surface acid sites are quite uniform.

The total number of acid sites may be determined by titration with NaOH of a weighed amount of solid acid containing 8.74% S. The titration result was 3.2 mmol/g. However, titration of the unsulfonated compound showed the presence of 0.7 mmol/g of phosphonic acid protons. The original unsulfonated solid contained 0.275 mol of the singly bonded phosphonic acid group or 0.55 mol of titratable protons. In terms of mmol/g, this

(26) Yang, C.-Y.; Clearfield, A. *React. Polym.* **1987**, *5*, 13.
(27) Haw, J. F.; Chuang, I. S.; Hawkins, B. L.; Maciel, G. E. *J. Am. Chem. Soc.* **1983**, *105*, 7206.
(28) Maciel, G. E.; Haw, J. F.; Chuang, I. S.; Hawkins, B. L.; Early, T. A.; McKay, D. R.; Petrakis, L. *J. Am. Chem. Soc.* **1983**, *105*, 5529.
(29) Xu, T.; Kob, N.; Drago, R. S.; Nicholas, J. B.; Haw, J. F. *J. Am. Chem. Soc.* **1997**, *119*, 12231.

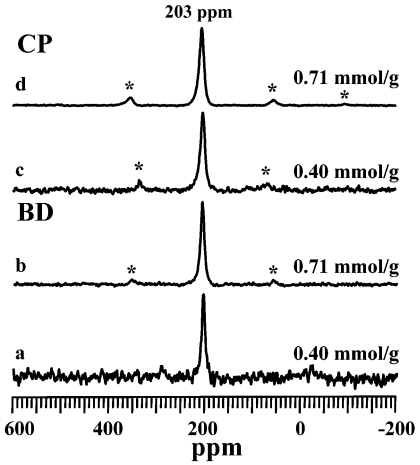

Figure 5. ^{15}N solid state NMR studies of pyridine-^{15}N on the **S−ZrBPBP** sample. Spectra a and b obtained were using Bloch decay excitation; spectra c and d were obtained using cross-polarization experiments. The asterisks represent spinning sidebands.

Scheme 1. Protonation of Acetone by Bronsted Acids

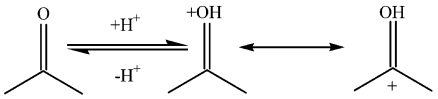

amounts to, assuming that both protons per free phosphonic acid were neutralized, 1.3 mmol/g. Apparently only half the protons were neutralized. The number of mmols of sulfonic acid groups is 3.2 minus the phosphonic acid titration value adjusted for the formula weight of the sulfonated product, or 0.56 mmol/g. This value is 2.64 mmol/g as compared to 2.77 mequiv/g based on sulfur content.

Determination of Acid Strength of −SO_3H in S-ZrBPBP. Our strategy to assess the acid strength of these porous sulfonated materials follows an NMR technique as developed by Haw et al.[30−32] applied mainly to zeolites. This method is a variable temperature solid state NMR approach for the in situ study of reactions between a solid acid and a sorbate. The sorbate contains a single carbon atom, highly enriched in ^{13}C. This carbon atom exhibits a considerable chemical shift from its normal resonance position upon interaction with the solid acid. They developed a scale of acid strengths based upon chemical shifts of known strong acids and superacids drawing upon work of Farcasiu et al.[33] For example, the isotropic chemical shift for acetone-2-^{13}C in 100% H_2SO_4 is 244 ppm from an original position of 205 ppm. The reaction responsible for this shift is given in Scheme 1. A listing of the chemical shifts for acetone-2-^{13}C as determined by Haw et al.[30,32] is given in Table 3.

Sulfonated zirconium biphenylenebis(phosphonate), sample number II-9 with 8.74% S, was examined by this technique, and the NMR spectrum of ^{13}C at low loading is shown in Figure 6. The chemical shift is seen to be 243 ppm, which is close to the shift of 100% H_2SO_4. The sharpness of the resonance indicates that the surface acidity is uniform. At the level of 0.47 mmol/g and room temperature, only small amounts of the condensation oligomerization products form. However, on heating to 80°C, several resonances barely visible in the room temperature spectrum increase in intensity. The small peaks in the 126−140 ppm region indicate the formation of aromatics from acetone. The peak at 191 ppm arises from the presence of acetic acid,[30] a cracking reaction product of diacetone alcohol. An additional cracking product of diacetone alcohol is isobutylene which in turn further reacts to yield aromatic products. Extensive condensation polymerization does not occur because of the low acetone loading. The first step in the presence of a strong Bronsted acid is protonation of the acetone molecule as shown in Scheme 1.

When the amount of acetone was increased to the saturation point, a more extensive number of products, and in greater quantities, formed. The NMR spectrum is shown in Figure 7. At this high concentration of acetone, the condensation−polymerization reactions are facilitated and are seen to occur readily at room temperature (Scheme 2). Water is formed during the condensation reactions, thereby decreasing the acidity of the solid catalyst. This results in the acetone-2-^{13}C resonance moving upfield to 221 ppm, which represents more moderate acidity, between that of zeolite HY and that of HZSM-5. That the mesityl oxide **1** peaks move to 211 (carbonyl) and 187 ppm (β-carbon) also shows that the surface acidity is now close to

Table 3. ^{13}C Chemical Shift of Acetone-2-^{13}C When Exposed to Different Acid Species

acid media	chemical shifts (ppm)	ref
$CDCl_3$	205	34
Ze-HX	215	30
Ze-HY	220	30
HZSM-5	223	30
H_2SO_4-80%	∼235	30
H_2SO_4-100%	244	35
$AlCl_3$	245	30
SO_3/H_2SO_4	246	30
FSO_3H/SbF_5	249	36, 37
SbF_5	250	30

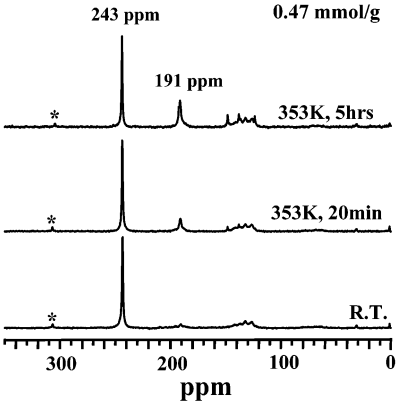

Figure 6. ^{13}C MAS NMR spectra of acetone-2-^{13}C adsorbed on the novel sulfonated zirconium phosphonate (**S−ZrBPBP**) sample ZKW-II-22. The asterisks represent spinning sidebands.

(30) Xu, T.; Munson, E. J.; Haw, J. F. *J. Am. Chem. Soc.* **1994**, *116*, 1962−1972.
(31) Xu, T.; Torres, P. D.; Beck, L. W.; Haw, J. F. *J. Am. Chem. Soc.* **1995**, *117*, 8027−8028.
(32) Haw, J. F.; Nicholas, J. B.; Xu, T.; Beck, L. B.; Ferguson, D. B. *Acc. Chem. Res.* **1994**, *29*, 259.
(33) Farcasiu, D.; Ghenciu, A.; Li, J.-Q. *J. Catal.* **1996**, *158*, 116.
(34) Breitmeier, E.; Haas, G.; Voelter, W. In *Atlas Carbon 13 NMR Data*; Heyden & Son, Ltd.: London, 1979.
(35) McClelland, R. A.; Reynolds, W. F. *Can. J. Chem.* **1976**, *54*, 718.
(36) Olah, G. A.; White, A. M. *J. Am. Chem. Soc.* **1968**, *90*, 1884−1889.
(37) Krivdin, L. B.; Zinchenko, S. V.; Kalabin, G. A.; Facelli, J. C.; Tufro, M. F.; Contreras, R. H.; Denisov, A. Y.; Gavrilyuk, O. A.; Mamatyuk, V. I. *J. Chem. Soc., Faraday Trans.* **1992**, *88*, 2459−2463.

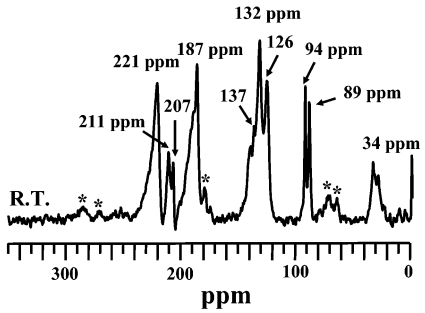

Figure 7. ^{13}C MAS NMR spectrum of acetone-2-^{13}C saturated on the novel sulfonated zirconium phosphonate (**S−ZrBPBP**) sample ZKW-II-22. The asterisks represent spinning sidebands.

Scheme 2. Condensation Polymerization of Acetone in the Presence of Strong Bronsted Acids[a]

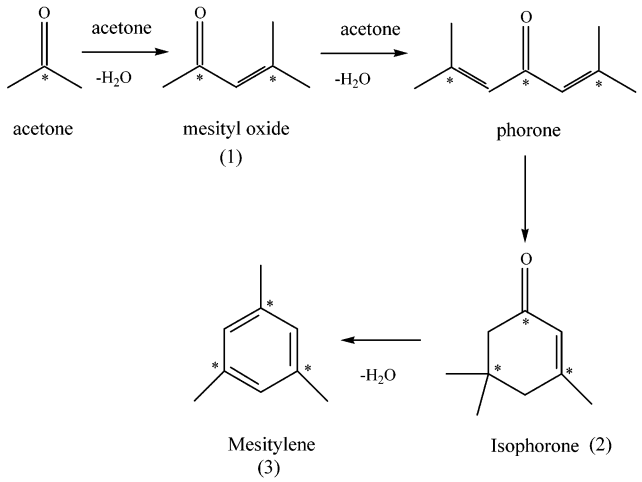

[a] The stars indicate the positions of the original ^{13}C.

that of HY. The peaks at 207 and 187 ppm are the chemical shifts of partially protonated carbonyl and β-carbon of isophorone (**2**), respectively, and the chemical shift of the third carbon of isophorone appears at 34 ppm. The shoulder peak at 137 ppm is evidence of formation of 1,3,5-trimethylbenzene (mesitylene (**3**)), and the region 126−140 ppm corresponds to aromatics and olefins. The "mysterious" peak at 94 ppm has been found when acetone reacts on zeolite HZSM-5, and it disappears at higher temperature (473 K).[30,38]

We propose that this species is surface bonded mesityl oxide **4**. The partially protonated carbonyl carbon bonds to the surface oxygen atom to form this species, and the chemical shift of the β-carbon moves back to the olefin region. The peak at 89 ppm is assigned to surface bonded isophorone **5**, whose chemical shift should be slightly smaller than the shift for surface bonded mesityl oxide. In addition, after the sample is heated at 353 K

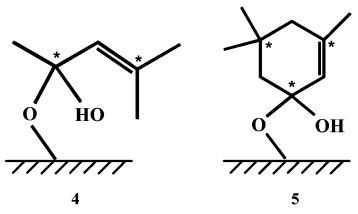

for 20 min, its NMR spectrum does not show a significant difference, only a slight decrease in the intensity of the acetone signal. This is an indication that the activation energies of these

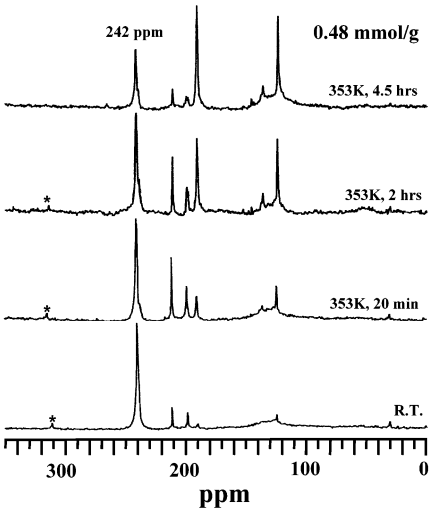

Figure 8. ^{13}C MAS NMR spectra of acetone-2-^{13}C adsorbed on the sulfonated zirconium phosphonate (**S−ZrTPBP**) sample ZKW-II-25. The asterisks represent spinning sidebands.

reactions are very low for acetone and, even at room temperature, reach equilibrium quickly. Therefore, both low loading and saturated acetone experiments demonstrate that the acid sites in this solid acid are very strong.

It was of interest to see how the acetone reaction would proceed on the highly sulfonated (15.5% S) zirconium terphenyl derivative. The NMR spectra are presented in Figure 8. The loading was the same, within experimental error, as that for the biphenylenesulfonate in Figure 6. The main resonance is at 242 ppm, essentially the same as for the biphenyl derivative, an indication that the acid strength is the same as the biphenyl derivative. The ^{13}C chemical shifts for the carbonyl carbon and the β-carbon of mesityl oxide appear at 212 and 199 ppm, respectively. The large downfield shift to 199 ppm for the β-carbon of mesityl oxide also suggests the very strong acidity of the catalyst. For comparison, the β-carbon of mesityl oxide in 100% H_2SO_4 was given as 203 ppm.[39] The intensity of the mesityl oxide first increases with reaction temperature and then decreases with reaction time, consistent with its being a reaction intermediate. The resonance at 191 ppm is due to formation of acetic acid[30] and its peak intensity increases dramatically with higher reaction temperature and time. Also, the amount of CO_2 obtained at higher temperatures also increases, produced through the decarboxylation of acetic acid. The other cracking product, isobutylene, also reacts further to form aromatic products (peaks in the 120−140 ppm region). The chief aromatic formed is at 121 ppm. The small peak at 137 ppm that emerges with time is due to formation of mesitylene. The greater amount of products obtained with the terphenyl derivative is undoubtedly due to the greater density of sulfonic acid groups, 1.32/ring, as compared to the biphenylene sulfonate (0.714/ring).

Cyclopentanone-1-^{13}C as a Probe Molecule. Cyclopentanone **6** undergoes condensation polymerization reactions similar to those of acetone but has a lower reactivity.[30] The most common reaction products are 2-cyclopentylidene-cyclopentanone **7** and trindane **8** with both **6** and **7** accepting protons

(38) Bosácek, V.; Kubelková, L.; Nováková, J. In *Catalysis and Adsorption by Zeolites*; Ohlmann, G., Pfeifer, H., Frickie, R., Eds.: Elsevier: Amsterdam, 1991; pp 337−346.
(39) Farcasiu, D.; Ghenciu, A.; Miller, G. *J. Catal.* **1992**, *134*, 115.

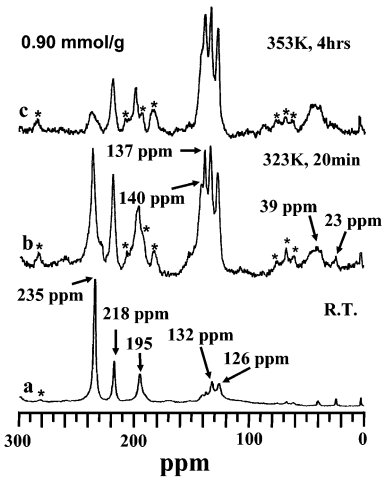

Figure 9. ^{13}C MAS NMR spectra of cyclopentanone-1-^{13}C adsorbed on the sulfonated zirconium biphenylenebis(phosphonate), sample II-22B (3.86%S): (a) loading of 0.32 mmol/g, at room temperature; (b) loading of 0.32 mmol/g, heated at 353 K for 24 h; (c) loading of 0.90 mmol/g heated at 353 K for 4 h. The asterisks represent spinning sidebands.

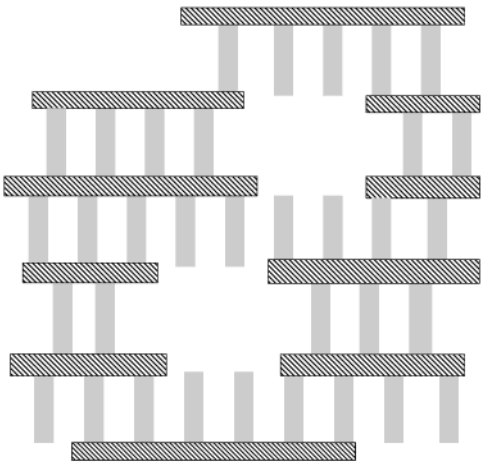

Figure 10. A schematic drawing of how micropores may develop in the zirconium biphenylenebis(phosphonate). The gray rectangles represent the biphenyl pillars, and the horizontal striped bars are the inorganic layers. The biphenyl groups bounding the pore are bonded to the layers through only one phosphonate group.

from strong acids. The catalyst used was sample II-9 with a

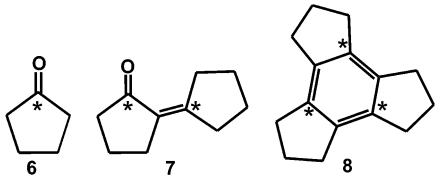

low level of sulfonation, 3.86% sulfur. At a low loading of 0.32 mmol/g, a number of products were formed even at room temperature (Figure 9a). Compound **7** is represented by two peaks at 218 ppm (carbonyl carbon) and 199 ppm (β-carbon), while the carbonyl carbon of **6** is represented by the peak at 239 ppm. The corresponding values for cyclopentanone in $CDCl_3$ and for the β-carbon of **7** are 217 ppm and 157 ppm. The large shift in these values on the sulfonate are indicative of high acid strength even at a low concentration of acid groups.

The peaks at 126, 132, and 140 ppm indicate the presence of olefins and aromatics. Upon raising the temperature to 353 K, the amount of compound **7** increases as do the olefins and aromatics (Figure 9b). Eventually, all the cyclopentanone is converted, and then the amount of **7** decreases as it further undergoes cracking reactions. A small amount of hydrocarbon was also formed, corresponding to peaks at 23 and 39 ppm. The sharp peak at 23 ppm could be a secondary reaction product, isobutane, which may evaporate at higher temperatures.

Increasing the loading of **6** to 0.9 mmol/g yielded a similar NMR spectrum as that obtained at the lower loading except that a small amount of trindane formed (137 ppm) in Figure 9b and c. The chemical shift for cyclopentanone-1-^{13}C (235 ppm) and that of the β-carbon of **7** (195 ppm) are at slightly lower values than in Figure 9a. This general lowering of the acidity may result from the generation of additional water at the higher loading. Increasing the temperature dramatically increases the amount of trindane as well as the peaks for aromatics and olefins. After the sample was heated at low temperature, 323 K, for a short time, the sample temperature was increased to 353 K and held for a longer time. The amounts of cyclopentanone **6** and compound **7** decreased, but the amounts of aromatics and olefins did not increase significantly. This indicates that the activation energies of the reactions are quite low, and just slight heating has a significant effect on the rates of the reactions. In addition, the formation of **8** is also evidence of the relatively larger micropores in this solid acid, compared to those in highly acidic zeolites.

The reaction of **6** at a loading of 0.36 mmol/g on the highly sulfonated terphenyl catalyst gave a shift of 253 ppm at room temperature. A small amount of **7** formed, and the carbon-13 peak positions were at 217 and 203 ppm. These much larger downfield shifts for the cyclopentadiene and β-carbon of **7** indicate an extremely high acidity for this catalyst. At 353 K, the amount of compound **7** increases and continues to increase with time. A small amount of trindane forms along with acetic acid (193 ppm) and olefins. The lack of significant product development despite the high acid strength, we attribute to the very high number of acid sites, about 15−16 per ketone molecule. Thus, the protonated species are far apart from each other reducing the amount of polymerization.

Discussion

An adequate model of the porous zirconium biphenylenebis(phosphonates) must be able to account for the following facts: (i) surface areas of 400 m^2/g; (ii) pores between 10 and 20 Å in diameter; (iii) ratios of P/Zr greater than 2; (iv) the role-played by fluorine; and (v) how micropores can form without spacer groups. A simple cartoon depiction of our proposed model is given in Figure 10. The inorganic $Zr(O_3P)_{2-}$ layers are depicted by the horizontal rectangular bars containing slanted lines. The biphenyl groups connecting the layers are represented by two parallel vertical lines. Those biphenyl groups bonded to only one layer are capped at the free end by a horizontal line that represents a free phosphonic acid group. The pores are formed during crystal growth by the coming together of layers of unequal length. Once cross-linking begins, these fragments are held in place, creating voids, as shown. These voids must follow a somewhat torturous path through the catalyst particle.

We assume that the layers have the same structure as those of zirconium phenylphosphonate.[15] This compound belongs to

the space group *C*2/*m*, which requires the metal atoms to lie in a plane and be six-coordinate. Each phosphonate group bonds to three metal atoms, forming an almost equilateral triangle, and the phenyl groups are ~5.3 Å apart. We therefore assume that the biphenyl groups are also 5.3 Å apart in adjacent positions. Because the X-ray powder pattern always indicates an interlayer spacing of ~14 Å for the biphenyl derivatives and 17.7 Å for the terphenyl compound, the model must reflect these spacings. Also, the presence of fluoride in the coordination sphere of Zr must be accounted for. Examples of fluoride ion singly bonded to Zr in zirconium phosphonates are known,[40] so we have assumed the same is true for the pillared porous compounds. However, some HF may be trapped in the pores and not washed out. This point needs further investigation. The inorganic prototype for these layered zirconium phosphonates is α-zirconium phosphate (α-ZrP).[13,14] We have shown earlier that crystals of α-ZrP grow very slowly. In fact, addition of phosphoric acid to Zr^{4+} results in precipitation of an amorphous gel, and this gel is only slowly converted to crystals by refluxing in excess H_3PO_4.[41,42] Refluxing the gel in 2.5 M H_3PO_4 for 15 h produces particles that are just beginning to take crystalline shape and are 50−70 nm in length. The mechanism of growth is Ostwald ripening as crystal growth accelerates with an increase in solubility, that is, an increase of H_3PO_4 concentration and temperature.[42] However, the cross-linked three-dimensional structure of the bisphosphonates is extremely insoluble in aqueous media producing totally amorphous particles. Addition of HF keeps the zirconium in solution as a hexafluoro anion that slowly releases the Zr(IV) at elevated temperatures. This is a form of homogeneous precipitation which produces some order in the particles and some particle growth. However, as we have shown, the individual particles are very small, but growth may occur by another mechanism. The bisphosphonates on the surface will have one end bonded and the other bonded with a free phosphonic acid group. These free acid groups may serve as nuclei for new particle formation but not necessarily covering the entire surface. Thus, the many intergrown particles appear at low magnification as a single large particle but, in essence, are a fusion of small particles. Our model differs from that of Alberti et al.[18] in that they assumed all the singly bonded biphenyl groups resided on the external surface and the particles were only a few layers thick. Our model predicts the presence of free phosphonic acid groups on the internal as well as the external surfaces. However, in Figure 10, we show that the external surfaces are smooth as though terminating with Zr atoms. This is partly correct because we used an excess of Zr in the synthesis, capping the layers with Zr.

It occurred to us that if an excess of Zr was added to the reactant mix, that the surface bonded biphenylenediphosphonate groups terminating the layers, which normally would project free phosphonic groups into space, would react to form smooth Zr terminated surfaces. However, such a surface would enhance particle growth in the same way that layer-by-layer, thin films are synthesized.[43] That is, the layers would continue to grow until one or the other reagent was depleted. By employing an excess of Zr, particle growth would continue until all the 4,4′-biphenylenediphosphonic acid was reacted. This procedure led directly to the microporous products of high surface area and narrow pore distribution as described here. There is also the possibility that HF in an organic polar solvent forms small micelle-like hydrogen bonded entities that template the layer growth. The fact that changing the solvent from pure DMSO to almost pure ethanol produces little change in the products in the case of the biphenyl derivatives vitiates against this idea. Additional particle growth studies are indicated and will be pursued.

Sulfonic acids of zirconium phosphonates are not new. Di Giacomo and Dines prepared 3-sulfopropylphosphonate, $Zr(O_3P(CH_2)_3SO_3H)_2$, starting with 3-bromopropylsulfonic acid and zirconium 2-(sulfophenyl)ethylphosphonate, $Zr(O_3PCH_2CH_2C_6H_4SO_3H)_2$, starting with the corresponding bromosulfonic acid. They demonstrated the ion exchange behavior and acidity of these compounds in a straightforward manner.[44]

Our own earlier studies on ion exchange[45] and conduction behavior of $Zr(O_3PC_6H_4SO_3H)_2$ [46] and those of Alberti and associates[47] are well documented. What is really novel is the porous nature of the pillared products. Recently, Curini et al.[48] prepared $Zr(O_3PCH_3)_{1.2}(O_3P-C_6H_4SO_3H)_{0.8}$ and tested it in several carbonyl regeneration reactions in solution. The large amount of methyl phosphonate groups was introduced into the catalyst to prevent the deliquescence of the pure sulfophenylphosphonate. The reactions were carried out with solutions of carbonyl compounds (oximes, semicarbazones, tosylhydrazones, dithiolanes, and ditheanes) in contact with the solid catalyst. Even in this highly diluted condition, the reactions proceeded smoothly, the catalyst was recovered by filtration, and the solutions worked up to recover the product. It is to be expected that the much higher acid strength of our porous sulfonates and the undiluted sulfophenylphosphonate will allow a wide range of acid catalyzed reactions to be effected under relatively mild conditions. Furthermore, given the adjustability of the pore dimensions as listed in Table 1, it should be possible to treat many large molecules that cannot access zeolite pores.

Acknowledgment. This study was supported with funds provided by NSF Grant No. DMR-0080040 and the Robert A. Welch Foundation Grant No. A673, for which grateful acknowledgment is made. This work made use of the Texas A&M University Department of Geology and Geophysics and Microscopy and Imaging Center. Thanks to Dr. Renald Guillemette for WDS−SEM measurements and Rick Littleton for the acquisition of SEM images. Zhike Wang would also like to thank Dr. Robert Taylor for help with NMR measurements.

JA030226C

(40) (a) Poojary, D. M.; Vemeulen, L. A.; Vicenzi, E.; Clearfield, A.; Thompson, M. E. *Chem. Mater.* **1994**, *6*, 1845. (b) Poojary, D. M.; Zhang, B.-L.; Clearfield, A. *J. Chem. Soc., Dalton Trans.* **1994**, 2453. (c) Poojary, D. M.; Zhang, B.-L.; Clearfield, A. *J. Chem. Soc., Dalton Trans.* **1994**, 2453.
(41) Clearfield, A.; Nancollas, G. H., Blessing, R. H. *Ion Exchange and Solvent Extraction*; Dekker, M. Inc.: New York, 1973; Vol. 5.
(42) Clearfield, A.; Thomas, J. R. *Inorg. Nucl. Chem. Lett.* **1969**, *5*, 775.
(43) Lee, H.; Kepley, L. J.; Hong, H.-G.; Akkter, S.; Mallouk, T. E. *J. Phys. Chem.* **1988**, *92*, 2597.
(44) DiGiacomo, P. M.; Dines, M. B. *Polyhedron* **1982**, *1*, 66.
(45) Kullberg, L.; Clearfield, A. *Solvent Extr. Ion Exch.* **1990**, *8*, 187.
(46) Stein, E. W., Sr.; Clearfield, A.; Subramanian, M. A. *Solid State Ionics* **1996**, *83*, 113.
(47) (a) Alberti, G.; Casciola, M.; Costantino, U. *Solid State Ionics* **1992**, *50*, 315. (b) Alberti, G.; Casciola, M.; Palombari, R. *J. Membr. Sci.* **2000**, *172*, 233.
(48) (a) Curini, M.; Marcotullio, M. C.; Pisani, E.; Rosati, O.; Costantino, U. *Synlett* **1997**, 769. (b) Curini, M.; Epifano, F.; Marcotullio, M. C.; Rosati, O.; Costantino, U. *Tetrahedron Lett.* **1998**, *39*, 8159−8162. (c) Curini, M.; Epifano, F.; Marcotullio, M. C.; Rosati, O.; Rossi, M. *Synth. Commun.* **2000**, *30*, 1319−1329. (d) Curini, M.; Epifano, F.; Marcotullio, M. C.; Rosati, O. *Synlett* **2001**, 1182−1184.